ECOLOGY

Impaired recovery of the Great Barrier Reef under cumulative stress

Juan-Carlos Ortiz[1,2*†], Nicholas H. Wolff[1,3,4*†], Kenneth R. N. Anthony[2], Michelle Devlin[5], Stephen Lewis[6], Peter J. Mumby[1,3†]

Corals of the Great Barrier Reef (GBR) have declined over the past 30 years. While reef state depends on the balance between disturbance and recovery, most studies have focused on the effects of disturbance on reef decline. We show that coral recovery rates across the GBR declined by an average of 84% between 1992 and 2010. Recovery was variable: Some key coral types had close to zero recovery by the end of that period, whereas some reefs exhibited high recovery. Our results indicate that coral recovery is sensitive to chronic but manageable pressures, and is suppressed for several years following acute disturbances. Loss of recovery capacity was partly explained by the cumulative effects of chronic pressures including water quality, warming, and sublethal effects of acute disturbances (cyclones, outbreaks of crown-of-thorns starfish, and coral bleaching). Modeled projections indicate that recovery rates can respond rapidly to reductions in acute and chronic stressors, a result that is consistent with fast recovery observed on some reefs in the central and southern GBR since the end of the study period. A combination of local management actions to reduce chronic disturbances and global action to limit the effect of climate change is urgently required to sustain GBR coral cover and diversity.

INTRODUCTION

The coral cover of many reefs has declined in the past few decades (*1*–*3*). Analyses of these trends have mostly attributed the loss of coral cover to major disturbances. Even on the extensively managed Great Barrier Reef (GBR), average coral cover has dropped by 50% in recent decades, a change that has been attributed to intense cyclones, outbreaks of crown-of-thorns starfish (COTS), and bleaching (*1*). While these recent disturbances have affected reef health, long-term changes in coral cover represent the balance of mortality from successive disturbances and recovery during intervening periods. Few studies have examined trends in the recovery side of this equation (*4*), even though reduction in recovery rates has been identified as a potential indicator of declining integrity of other ecosystems (*5*).

Here, we calculated coral recovery rate on the GBR (Fig. 1) from more than 1300 post-disturbance trajectories of coral taxa from 81 reefs over 19 years. We explore temporal and spatial trends in recovery rate and potential factors driving the observed patterns. In the second part of the study, we use an ecosystem model that includes demographic processes (recruitment, partial mortality, and growth) to explore potential ecological mechanisms driving the observed changes in recovery.

Recovery rate refers to the ability of a system to recover after disturbance. Here, it specifically refers to the rate at which the cover of a particular coral type changes after a perturbation (reduction in coral cover) (Fig. 1). Many population-level processes can influence recovery, including recruitment, colony somatic growth, and natural partial mortality. Corals were grouped into six categories based on a combination of taxonomy and functional traits (Table 1). Recovery trajectories were defined as intervals free of acute disturbance and as processes that begin either after a significant decline in coral cover or at the beginning of the time series (Fig. 1). Instantaneous growth rate (IGR) was used as the metric of recovery and was calculated for each recovery trajectory and each coral type.

RESULTS AND DISCUSSION

The average recovery rates of six major coral groups declined significantly over the study period, with reductions ranging from 68 to 143% (that is, including transitions from positive to negative growth rates, indicating net decline in coral cover between disturbances). Two of the coral groups—branching *Acropora* and *Montipora*—had negative average recovery rates by the end of the study period (2010; Fig. 2). Trends in recovery rate varied considerably across the GBR, and not all reefs showed declines (Fig. 3). In most cases, recovery rates were less negatively affected in the mid-northern and Swains region of the GBR (Fig. 3). This pattern is consistent with recent recoveries observed in these regions (*6*).

Although this is the first study to quantify a region-wide reduction in coral recovery rate, an impairment to reef recovery was first indicated during a study of COTS impacts on the GBR between 1985 and 1996 (*7*). This early study did not investigate potential drivers of the change, and it is challenging to identify mechanisms occurring at these large scales and in these complex ecosystems. It is possible, however, that acute disturbances may have legacy effects that impair subsequent recovery, as has been suggested after the 2002 bleaching event of the GBR (*8*).

Given the difficulty in providing an unequivocal account of mechanisms without the aid of large-scale—and prohibitively difficult—experimental manipulations, we take three approaches to provide some insight into potential causality. First, we use the conventional statistical approach of examining the explanatory power of drivers or measurable proxies. Drivers were selected where reasonable expectations of an effect on coral recovery were expected and included both top-down and bottom-up mechanisms (for example, legacy effects of disturbances and water quality, respectively). We did not include larval connectivity because of the uncertain coral population status of >95% of source reefs over time and the lack of larval connectivity metrics for the duration of monitoring (1992–2010; connectivity metrics are available from 2010 to

[1]Marine Spatial Ecology Lab, School of Biological Sciences, University of Queensland, St Lucia, Queensland 4072, Australia. [3]Australian Research Council Centre of Excellence for Coral Reef Studies, University of Queensland, St Lucia, Queensland 4072, Australia. [4]Global Science, The Nature Conservancy, Brunswick, ME 04011, USA. [2]Australian Institute of Marine Science, PMB3, Townsville, Queensland 4810, Australia. [5]Centre for Environment, Fisheries and Aquaculture Science, Lowestoft NR33 0HT, UK. [6]Catchment to Reef Research Group, Centre for Tropical Water and Aquatic Ecosystem Research, James Cook University, Townsville, Queensland 4811, Australia.
*These authors contributed equally to this work.
†Corresponding author. Email: j.ortiz@uq.edu.au (J.-C.O.); nicholas.wolff@tnc.org (N.H.W.); p.j.mumby@uq.edu.au (P.J.M.)

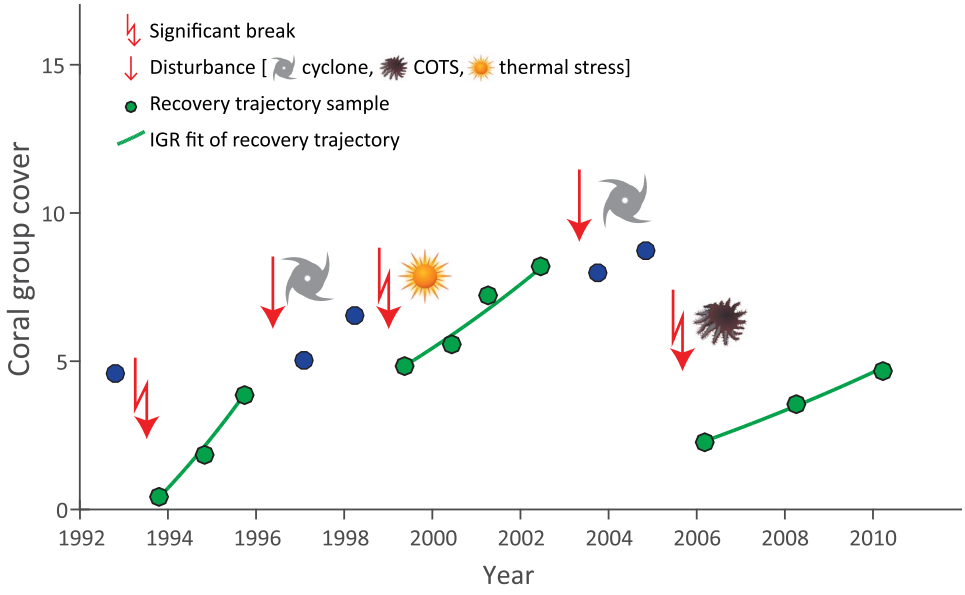

Fig. 1. A schematic to illustrate how recovery trajectories were defined for each of the six coral groups. Points represent observed coral cover through time. Green points are samples within recovery periods, and blue points are observations outside of recovery periods. Recovery trajectories begin at either the beginning of the time series or after a significant break (decline). Recovery trajectories end with either an acute disturbance (COTS, cyclones, or thermal stress), a significant break, or the end of the time series. The IGR for each recovery trajectory is calculated. Note that not all significant breaks were explained by acute disturbances. The examples of coral cover trajectories for each coral type are shown in the Supplementary Materials. COTS, cyclone, and sun symbols are from T. Saxby (Integration and Application Network, University of Maryland Center for Environmental Science; http://ian.umces.edu/imagelibrary/). COTS, crown-of-thorns starfish.

Table 1. Summary of permutational linear models. Multiple regressions were performed using 13 predictors and IGR as the response variable. All possible combinations of variables were explored, and AIC (Akaike information criterion) was used to select the most parsimonious model (with a difference of at least 2 units). Red signifies a negative relationship, blue signifies a positive relationship, and pink represents cases where the time no longer explained residual variance once other covariates were added to the model. Cell values give the relative contribution of each predictor to the total variance explained by the model (R^2). ns, nonsignificant effect.

Category of predictor	Predictor	Branching *Acropora*	Digitate *Acropora*	Tabular *Acropora*	*Montipora*	Pocilloporids	Massives
Temporal	Time			0.01	0.08		0.45
Spatial	Longitude	0.13	0.18	0.16	0.09	0.15	0.18
	Latitude	0.22	0.23	0.17	0.11	0.24	0.07
Ecological	Initial cover	0.31	0.25	0.54	0.28	0.25	0.13
	Macroalgal cover	0.09	ns	ns	ns	ns	ns
Water quality	Distance to river	ns	ns	ns	ns	ns	ns
	Flow during recovery	0.17	0.16	0.04	0.03	0.02	0.08
	Flow pre-recovery	ns	ns	ns	ns	ns	0.08
COTS	Pre-recovery density	ns	ns	ns	0.24	ns	ns
Cyclones	Pre-recovery maximum wind stress	ns	0.17	ns	ns	0.12	0.04
	Pre-recovery # events	ns	ns	ns	ns	0.21	ns
Thermal stress	Chronic during recovery	ns	ns	ns	ns	ns	ns
	Chronic pre-recovery	0.08	ns	ns	0.16	ns	0.03
	Acute pre-recovery	ns	ns	0.08	ns	ns	ns
	R^2	0.20	0.13	0.15	0.14	0.17	0.20

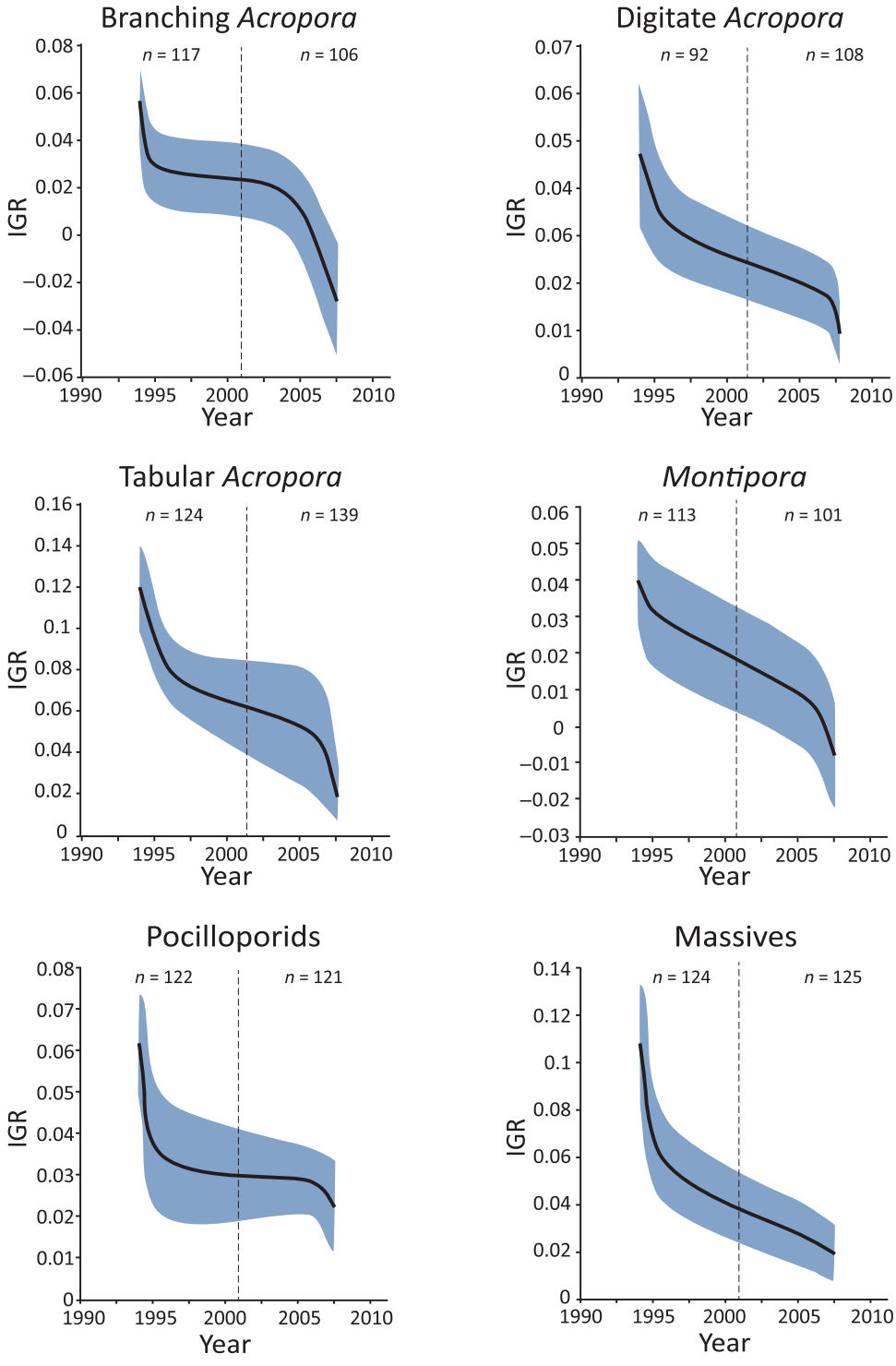

Fig. 2. Temporal trends in the IGR of major coral taxa on the GBR. Solid lines represent the mean, and blue areas indicate the SE. Dashed lines denote mean midpoints of the recovery trajectories. *n* values represent the number of trajectories before and after the mean trajectory midpoint. Note different scales on the *y* axes.

2016). Before statistical model selection, we verified that time was a significant predictor of recovery rate when used in isolation, that is, establishing that the recovery trends were real and not an artifact of, for example, varying intervals between disturbances. We then identified the most parsimonious model and found that a combination of five to seven predictors—depending on coral type—explained in total between 13 and 17% of the variability in recovery rate (Table 1). A combination of these predictors accounted for the temporal trend in half of the coral groups (branching *Acropora*, digitate *Acropora*, and pocilloporids), whereas time as a factor explained a residual level of variability in the remainder, implying a greater level of uncertainty in the drivers of temporal trends in tabular acroporids, *Montipora*, and massive corals

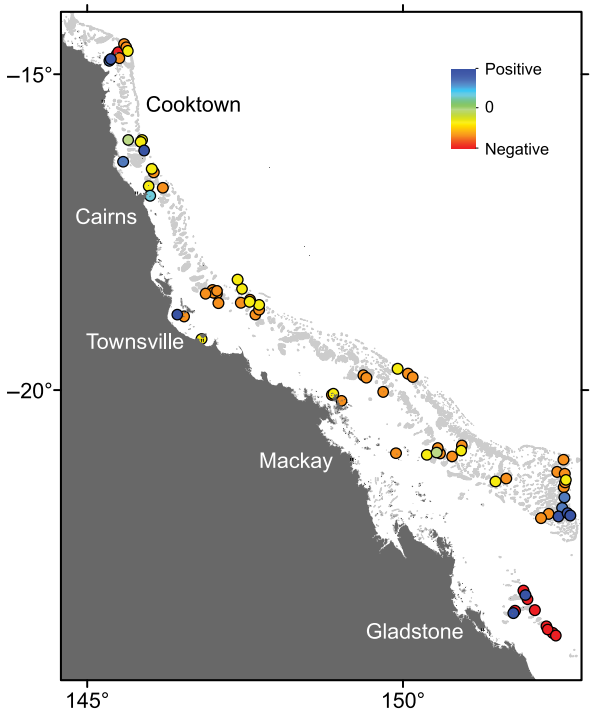

Fig. 3. Spatial distribution of change in reef recovery rates (IGR) for tabular corals of the genus *Acropora*. We chose tabular *Acropora* here because it is the dominant coral group (by abundance and frequency) and alone represents 30% of mean total coral cover of the groups we include. In addition, it has the largest number of recovery trajectories. Colors represent change in IGR between the first half and second half of the data set. Recovery trajectories were divided between two time periods, so temporal differences could be calculated: The earlier half included 131 recovery trajectories that all ended by 2003 with a mean trajectory midpoint of year 1995; the latter half included 132 trajectories that all ended after 2005 with a mean midpoint of 2007. Temporal change in IGR was calculated per reef [(later − earlier)/earlier] using mean IGR for cases where a reef had multiple trajectories per time period. In the cases where a reef did not have a value for the before or after period, inverse distance weighted interpolation was used to obtain the corresponding value. An autocorrelation analysis that evaluates the appropriateness of the interpolation is shown in the Supplementary Materials.

(Table 1). In every case, the total annual river flows to the GBR lagoon during the recovery period were found to be a relatively strong predictor, accounting for up to 17% of the explained variance. River flows were negatively related to recovery of all but one coral group (massive corals).

The history of disturbances before the onset of recovery suggests latent effects (Table 1). For example, the recovery of digitate *Acropora* corals was slower after stronger cyclones, which cause more significant damage to reefs (*9*). More powerful storms lead to increased fragmentation of coral rubble, which might extend the time needed for consolidation into the reef matrix, thereby delaying recovery. Our results reveal differential susceptibility of coral types to the different stressors. The recovery of digitate acroporids and pocilloporids is particularly sensitive to physical damage, while branching and tabular acroporids are sensitive to chronic effects of thermal stress. This differential susceptibility is likely to be driven by the specific combinations of life traits that these coral types have.

Statistical analysis quantifies the associations between recovery rate and available explanatory variables, but a number of feasible mechanisms cannot be investigated using this approach because data are not available. For example, coral recovery rates are likely to decline if rates of recruitment and growth decrease and partial mortality increases, yet these metrics are rarely measured in large-scale monitoring programs (*10*).

Moreover, given the observed marked reduction in recovery rate, we questioned whether these declines are consistent—or even feasible—given our current understanding of stressor impacts. To address this, our second analysis used a field-validated simulation model of coral community dynamics (*11*) to ask whether documented declines in coral vital rates driven by the stressors studied here could explain the observed declines in population recovery rate.

We found that 80% reductions in recovery rate (like those observed) could be the consequence of documented cumulative effects of stressors on coral recruitment, growth, and partial mortality. For example, the model indicates that the observed reductions in recovery could result from 55 and 27% reductions in both coral recruitment and somatic growth rate for tabular acroporids and massive corals, respectively (Fig. 4). Taking recruitment rate first, recent studies have documented positive stock-recruitment relationships for both brooding (*12*) and broadcasting coral species (*13*). Given the widespread loss of adult corals on the GBR (*1*), these positive stock-recruitment relationships could, if consistent throughout the GBR, potentially reduce recruitment rates by 22 to 78%, which encompass the level predicted by our model. Moreover, recruitment might decline in response to sublethal effects of thermal stress, which can reduce fecundity by up to 35% and persist for several years (*14*). Last, nutrient and sediment enrichment of GBR waters can impede coral larval settlement and recruitment because of interactions with benthic algae (*15*) and sediment (*16*, *17*).

Coral growth rates can decline for many reasons. Rates of calcification and growth have declined by 14% in some species, such as *Porites*, in response to rising thermal stress (*18*). Further, ocean acidification is likely to have reduced net reef calcification on the southern GBR corals (*19*). Growth can also be depressed for several years after bleaching events (*20*), and some corals shuffle their symbiont populations during thermal stress events, increasing the abundance of thermally tolerant symbiont types (*21*). While these symbionts can tolerate high temperatures, their dominance can reduce the growth of their coral hosts by up to 70% (*22*, *23*). Last, episodic coral diseases can reduce the net growth rates of some corals on the GBR (particularly tabular acroporid corals) by up to 21% (*24*, *25*). Again, an overall reduction in growth rate of 20 to 55% under cumulative pressures is not unrealistic.

We emphasize that our results do not constitute evidence that coral recruitment and growth rates on the GBR have declined. However, our model analysis provides plausible, mechanistic explanations for what might be driving the striking reductions in coral recovery we observe. Because of the complex, nonlinear, and interacting processes driving coral reef dynamics, each component process (for example, recruitment, somatic growth, and disease) need suffer only comparatively small change (for example, 27%) to result in the large reductions in recovery we document.

Our third approach was to identify and test for multiple potential confounding effects that could feasibly influence our results or interpretation. These effects included an increase in the frequency of disturbances over time, changes in the accuracy of survey data over time, changes in the durations of recovery trajectories, and inclusions of new sites in later years. In all cases, our tests for confounding effects were rejected, implying that our inferences are robust (section S1, tables S1 and S2, and fig. S1).

Several types of disturbance, including cyclones, occur in clusters: periods of intense activity that are followed by longer benign periods (*26*, *27*). Positing that recent decades might constitute a period of

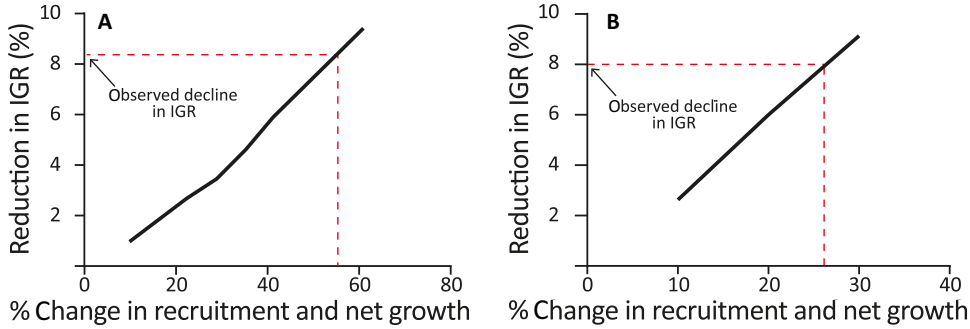

Fig. 4. Predicted sensitivity of recovery rate (IGR) to reduced coral recruitment and net growth. (**A**) tabular acroporids and (**B**) massive corals. IGR values (*y* axis) were calculated based on results of simulations using specific values of somatic growth and recruitment (*x* axis).

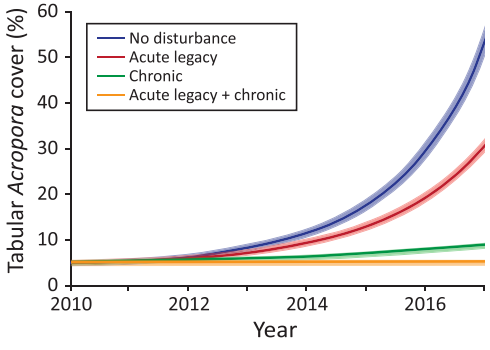

Fig. 5. Projected recovery after the study period under different disturbance scenarios. We use here Penrith Reef (a mid-shelf reef in the southern GBR) as example (see fig. S2 for examples from other reefs). Lines show the projected coral cover at the reef based on the IGR predicted from the statistical model. Shaded ribbons shows variability when the parameters are varied by 5%.

exceptionally high disturbance, we used our statistical model to explore the consequences of a "return" to less frequent disturbance in the future (Fig. 4). Covariates included geographic location (section S2 and fig. S2), an initial coral cover of 5% in year 2010, and various levels of chronic and acute disturbances (Fig. 5). Our statistical model showed that reefs could recover rapidly to a coral cover of 70% within 7 years if the legacy effects of acute disturbances and the intensity of chronic disturbances are reduced (Fig. 5). These recovery rates are similar to recent observations from southern portions of the offshore GBR, where effects of reduced water quality are minimal and there have been no acute disturbances in recent years (*6*). In contrast, the model showed that continued legacy effects of acute disturbance and/or strong chronic stress would severely stunt recovery potential (Fig. 5). These transient legacy effects could include reduced coral calcification and growth that persists for up to several years after bleaching events (*20*).

The response of coral reefs to natural and anthropogenic pressures is complex and is often described with an overly simplified metric of reef state such as total coral cover. Here, we go beyond a reef state characterization in our effort to quantify a critical functional response of the system: its recovery ability. We recognize up front that coral reef response is multivariate and that different components of the reef community are unequally affected by stresses. Accordingly, we examined six functional components of the coral assemblage and quantified their recovery ability independently. This allowed us to evaluate which parts of the coral community are more sensitive to cumulative pressures. While we believe that this novel analysis offers important new insights, we also acknowledge that there are many components of coral reef communities that are not considered here. For example, fish and invertebrate (other than coral) assemblages likely affect coral reef responses to disturbance.

The decline in average coral recovery rates is cause for concern, particularly in tabular and digitate corals, which play a disproportionately important role in driving reef dynamics (*11*). Moreover, with increasing frequencies and intensities of disturbances, any reduction in recovery rate may facilitate the ratcheting down of average reef state. As identified in our results, climate change is already affecting coral recovery rate both chronically and through the legacy effect of acute thermal events. Our analysis suggests that recovery rates are expected to decline further under climate change and ocean acidification because of impacts on coral recruitment and growth (*8*, *28*). Thus, we echo many other calls for urgent action to mitigate greenhouse gas emissions and maintain functioning ecosystems. However, while we anticipate that average coral cover will decline, the striking spatial variability in recovery rate implies that some reefs will continue to function far better than others. Understanding the causes of this variability is important and will help target management actions and the delivery of ecosystem services through the identification of reefs/regions, where the ecological benefits of local management action can be maximized. A considerable amount of variance was explained by proxies of water quality. Because water quality can be improved through management and policy, and is the focus of continued government investments (*29*), its deleterious influence on coral recovery may weaken in future. The emerging picture is one of substantial heterogeneity that requires carefully tailored management interventions and renewed action on global scales.

MATERIALS AND METHODS

Sampling summary

For this analysis, we used 279 sites from 93 reef locations (3 sites per reef) that together form the Australian Institute of Marine Science (AIMS) Long-Term Monitoring Program (LTMP) (Fig. 3). For 47 reefs, sampling began approximately in 1992 (but initial visits ranged from 1992 to 1995). An additional 46 reefs were added to the program in 2005/2006. Sampling occurred approximately annually through 2004, but when the additional reefs were added, reef sampling occurred approximately every 2 years to accommodate all reefs. This analysis encompasses the years 1992 (sampling began) to 2010 (the extent of some of our environmental variables) for a total of 2565 site visits (855 reef visits).

Sampling protocol

Each site has five permanent (5 m × 50 m) transects that are photographed (40-cm distance) at approximately 1-m intervals. Percentage cover of corals and other benthic categories are estimated from five points in each image, so approximately 200 systematically dispersed points are sampled from each transect. Hard coral, the focus of this analysis, are identified to the genus level, where possible.

Dependent variable (population growth rates)

Coral taxa

Coral were grouped into six morphological categories: branching *Acropora*, digitate *Acropora*, tabulate *Acropora*, *Montipora*, Pocilloporidae, and massives (Table 1). Together, these groups represent more than 80% of GBR coral cover while also having distinct life history traits that likely influence recovery rate (*11*). The massives group included several genera (for example, Favia, Favites, Porites, and Goniopora). The mean cover of each group was calculated per site and sampling period, and this served as the basis for all analyses. In the case of massive corals, we combined all (*16*) genera to ensure enough recovery periods for the analysis. The functional role of massive corals is relatively similar among genera and different to the role of the other coral types studied.

Analysis—Statistical breaks and recovery trajectories

For each taxonomic group, a paired *t* test of transect data was used to determine whether there was a statistical break (significant decline) in coral cover between successive visits to each site. Paired *t* test was justified because each transect was permanent and uniquely identified. As each *t* test was independent and the interpretation of multiple *t* tests was not used for statistical inference, error accumulation is not a concern in this analysis.

To construct recovery trajectories for each taxon/site combination during periods with no disturbances, we used the following criteria: A recovery trajectory began with either the first sample for a site or the second (lower) of the two samples that defined a statistical break. Trajectories continued until either the end of the time series (approximately 2010), or until the first (higher) of the two successive samples that defined a statistical break, or until a disturbance was noted at the site. A trajectory was defined by a minimum of two successive samples with a maximum of the entire time series in cases where there were no significant breaks. The average number of visits per trajectory was three with duration raging between 1 and 14 years. Twelve reefs that had no periods of time met these criteria and were excluded, and therefore, the final number of reefs used for the analysis was 81.

Calculating IGR

We used the IGR of coral recovery trajectories as the response variable in our analyses. Here, recovery trajectories were assumed to follow an exponential curve. An advantage of assuming exponential growth is that the IGR provides a single metric that can be calculated with as few as two points and is independent of recovery duration. This is important given that recovery durations varied widely among sites. We recognize that a shortcoming of this approach is that coral reef growth likely slows as carrying capacity is approached and that the full scope of recovery is therefore better described by logistic growth. However, fitting our data with logistic growth would require its own limitations, such as assumptions about carrying capacity (k) and sigmoid midpoint (x_o), which may vary in space and time. Further, because the two approaches are similar while coral cover remains low (that is, the exponential component of logistic growth) and because most of our recovery trajectories begin at low coral cover and are relatively short (the mean duration was 3 years), we suspect that the carrying capacity issue is minor in our analysis. To help mitigate this potential confounding effect, we included initial coral cover in all the models as a covariate. Finally, we opted to use end points to calculate IGR because we considered the outcome of the recovery period (the final measurement) to be a more important indicator of reef performance than mean performance over the entire period. However, IGR estimates were very similar whether calculated using end points or exponential fits of all sample points (see the Supplementary Materials).

IGR (=r) was calculated using the exponential growth Eq. 1 for each recovery trajectory

$$N_{t+1} = N_t x e^{rt} \quad (1)$$

where $N_{(t+1)}$ is percent cover at time $t+1$, $N_{(t)}$ is percent cover at time t, r is the instantaneous recovery rate, and t is time in years. Solving for r, the equation in practice was used as follows:

$$r = \ln[(N_{t+1} + 5)/(N_t + 5)]/((t+1) - t) \quad (2)$$

Note that a value of 5% was added to all coral cover to avoid arbitrarily low (or high) IGRs when coral cover approaches zero and to solve issues arising from when coral cover actually equaled zero. The IGR was calculated using the end points of each trajectory.

Independent variables (disturbances)

To analyze the impact of disturbance on IGR, we distinguished between two broad mechanisms: (i) Chronic (press-type) stressors that occur during a recovery trajectory could act to increase mortality, retard growth, or depress recruitment, or all; (ii) acute (pulse-type) disturbances that occur before a recovery trajectory may have ongoing sublethal legacy effects such as reductions in recruitment success due to loss of consolidated substrate after cyclones, reductions in growth rate and fecundity after acute thermal stress, and increased susceptibility to disease.

Cyclones (two variables)

Individual cyclone tracks were downloaded from the Australia Bureau of Meteorology (BoM) for the years 1991–2010. These data include cyclone eye location and maximum wind, recorded generally every 6 hours. Maximum winds were categorized according to the BoM cyclone intensity scale (1 to 5). Using geographic information system (GIS), the spatial extent of winds of different categories was estimated using asymmetric buffers (*27*). The maximum category experienced at each LTMP site from each cyclone was then extracted.

Any cyclone (category ≥ 1) that intersected a site was considered a major disturbance and consequently met the criteria for terminating the recovery trajectory. Thus, the sample just before the cyclone was considered the last time point of the trajectory. For each recovery trajectory, two metrics of cyclone activity before the recovery were included in the statistical analysis: the total number of cyclones (count) and the maximum wind stress (Pa) experienced at each site. Wind stress was calculated using an empirical formula based on wind speed (minimum associated with each cyclone category), surface air density, and sea surface drag coefficient (*30*).

Chronic and acute sea surface temperature (three variables)

Sea surface temperature (SST) and derived thermal metrics were extracted for the GBR from version 4 of the National Oceanic and Atmospheric Administration (NOAA) Coral Reef Temperature Anomaly Database (CoRTAD) (*31*). These weekly 4 km × 4 km resolution data cover the years 1982–2010. Two thermal stress metrics based on degree heating weeks (DHWs) were used in this analysis: DHW_{acute} and $DHW_{chronic}$. DHW_{acute} represents the magnitude and duration of thermal stress above the observed maximum weekly climatological SST at a given site. DHW_{acute} was derived using the methods adopted by NOAA Coral Reef Watch, which accumulates any hot spots >1°C over a 12-week window (*32*). DHW_{acute} is associated with bleaching and possible proceeding mortality and only occurs during summer months. $DHW_{chronic}$ is estimated in a similar fashion as DHW_{acute}, except using mean (instead of maximum) weekly climatological SST. Often, $DHW_{chronic}$ is significant in years with low or no DHW_{acute} and, unlike DHW_{acute}, can occur any time of the year. $DHW_{chronic}$ is analogous to the SST anomaly DHW metric captured within CoRTAD (*31*).

A DHW_{acute} of greater than 4 degree-heating-weeks, a threshold above which some reefs will start to bleach (*32*), was considered a major disturbance and consequently met the criteria for terminating a recovery trajectory. In addition, for each recovery trajectory, two metrics of thermal stress before the recovery (to measure legacy effects) were included in the statistical analysis: the maximum DHW_{acute} and maximum $DHW_{chronic}$. Finally, the mean $DHW_{chronic}$ was recorded as a potential stressor during each recovery trajectory and included in the statistical analyses.

Crown-of-thorns-starfish (one variable)

COTS densities were estimated from manta tow surveys conducted by AIMS around the perimeters of the reefs used in this analysis for the years 1992–2010 (*33*). COTS densities of one or more per manta tow were considered active outbreaks and thus a major disturbance justifying the termination of a recovery trajectory (*33*). In addition, we included the maximum COTS density before every recovery trajectory as an independent variable in our statistical analysis to account for legacy effects of COTS outbreaks on coral cover.

Water quality (two variables)

Because of human land use, runoff from catchments is a significant threat to the GBR (*29*). The magnitude and extent of riverine plumes (and load of associated pollutants) are highly correlated with wet-season discharge (*16*, *17*, *34*). Here, we used metrics of GBR-wide river discharge as proxies for water quality effects. We included total wet-season river discharge both before and during each recovery trajectory as a potential chronic stressor in the statistical analyses.

Distance from river mouth (one variable)

The distance from each site to the closest of the main influential GBR rivers was recorded as an explanatory variable (*35*).

Spatial coordinates (two variables)

The *X* and *Y* coordinates from the Universal Transverse Mercator (UTM) projection were included as two static explanatory variables, representing latitude and longitude.

Initial coral cover (one variable)

For each coral taxon, the initial coral cover for each recovery trajectory was included as an explanatory variable.

Average macroalgal cover as a proxy for herbivory

Average macroalgal cover was calculated per trajectory. Macroalgae can influence coral recruitment, growth, fecundity, and mortality, and trends might reflect changes in nutrient concentration or herbivory.

Time (one variable)

The midpoint (in years) of the recovery trajectories was used as an indicator of time.

Statistical approach

To explore temporal and spatial patterns in coral IGR as well as potential drivers of these patterns, multiple general linear models were constructed for each coral group. Permutations were used to determine the statistical significance of each model. Each model contained latitude, longitude, and time to ensure that the spatial and temporal structure of the data set was considered in all models. All possible combinations of the remaining 13 explanatory variables and these 3 fixed ones were explored. AIC was used to determine the most parsimonious model for each coral group, ensuring that a difference of at least 2 units of AIC was present. To avoid multicollinearity among response variables, we checked the correlation coefficient of each pair of variables. Only variables with less than 50% correlation were included in the models.

SUPPLEMENTARY MATERIALS

Supplementary material for this article is available at http://advances.sciencemag.org/cgi/content/full/4/7/eaar6127/DC1

Section S1. Exploration of potential confounding effects on the observed patterns in coral recovery rate

Section S2. Projected recovery of reefs in different regions of the GBR as a function of different disturbance regimes

Section S3. Comparing IGR estimates

Section S4. Identification of recovery periods

Section S5. Spatial autocorrelation of reef IGR

Table S1. Summary of the six permutation-based linear mixed models performed to check the effect of within-site versus between-site variability on the observed reduction in IGR.

Table S2. Summary of the six permutation-based linear mixed models performed to check the effect of the inclusion of the new reefs [reef types with two levels (original and new)] on the observed reduction in IGR.

Table S3. Summary of the six permutation based linear models performed to check for the effect of the different starting points for each recovery trajectory [trajectory type with two levels (starting with first visit or starting after reduction in coral cover)] on the observed reduction in IGR.

Fig. S1. Small but significant differences in coral cover (less than 3%) plotted against time.

Fig. S2. Projected recovery after the studied period under different disturbance scenarios for three GBR reefs (Linnet Reef in the northern, Kelso Reef in the central, and Penrith Reef in the southern part of the GBR).

Fig. S3. For this study, we calculated the IGR of recovery periods (n = 1392) using recovery trajectory end points (first and last).

Fig. S4. Example time-series for each of the six taxa groups explored here.

Fig. S5. Semivariogram of reef tabular *Acropora* IGR.

REFERENCES AND NOTES

1. G. De'ath, K. E. Fabricius, H. Sweatman, M. L. Puotinen, The 27–year decline of coral cover on the Great Barrier Reef and its causes. *Proc. Natl. Acad. Sci. U.S.A.* **109**, 17995–17999 (2012).
2. J. F. Bruno, E. R. Selig, Regional decline of coral cover in the Indo-Pacific: Timing, extent, and subregional comparisons. *PLOS ONE* **2**, e711 (2007).
3. T. A. Gardner, I. M. Côté, J. A. Gill, A. Grant, A. R. Watkinson, Long-term region-wide declines in Caribbean corals. *Science* **301**, 958–960 (2003).
4. K. Osborne, A. M. Dolman, S. C. Burgess, K. A. Johns, Disturbance and the dynamics of coral cover on the Great Barrier Reef (1995–2009). *PLOS ONE* **6**, e17516 (2011).
5. M. Scheffer, J. Bascompte, W. A. Brock, V. Brovkin, S. R. Carpenter, V. Dakos, H. Held, E. H. van Nes, M. Rietkerk, G. Sugihara, Early-warning signals for critical transitions. *Nature* **461**, 53–59 (2009).

6. Australian Institute of Marine Science, *Condition of Great Barrier Reef Corals Before the Mass Bleaching Event in 2016* (Australian Institute of Marine Science, 2016); www.aims.gov.au/-/05-april-condition-of-great-barrier-reef-corals-before-the-mass-bleaching-event-in-2016.
7. R. M. Seymour, R. H. Bradbury, Lengthening reef recovery times from crown-of-thorns outbreaks signal systemic degradation of the Great Barrier Reef. *Mar. Ecol. Prog. Ser.* **176**, 1–10 (1999).
8. K. Osborne, A. A. Thompson, A. J. Cheal, M. J. Emslie, K. A. Johns, M. J. Jonker, M. Logan, I. R. Miller, H. P. A. Sweatman, Delayed coral recovery in a warming ocean. *Glob. Chang. Biol.* **23**, 3869–3881 (2017).
9. M. Puotinen, J. A. Maynard, R. Beeden, B. Radford, G. J. Williams, A robust operational model for predicting where tropical cyclone waves damage coral reefs. *Sci. Rep.* **6**, 26009 (2016).
10. J. Flower, J.-C. Ortiz, I. Chollett, S. Abdullah, C. Castro-Sanguino, K. Hock, V. Lam, P. J. Mumby, Interpreting coral reef monitoring data: A guide for improved management decisions. *Ecol. Indic.* **72**, 848–869 (2017).
11. J.-C. Ortiz, Y.-M. Bozec, N. H. Wolff, C. Doropoulos, P. J. Mumby, Global disparity in the ecological benefits of reducing carbon emissions for coral reefs. *Nat. Clim. Chang.* **4**, 1090–1094 (2014).
12. C. Doropoulos, S. Ward, G. Roff, M. González-Rivero, P. J. Mumby, Linking demographic processes of juvenile corals to benthic recovery trajectories in two common reef habitats. *PLOS ONE* **10**, e0128535 (2015).
13. L. Bramanti, P. J. Edmunds, Density-associated recruitment mediates coral population dynamics on a coral reef. *Coral Reefs* **35**, 543–553 (2016).
14. S. Ward, P. L. Harrison, O. Hoegh-Guldberg, Coral bleaching reduces reproduction of scleractinian corals and increases susceptibility to future stress, in *Proceedings of the 9th International Coral Reef Symposium*, Bali, Indonesia, 23 to 27 October 2000, pp. 1123–1128.
15. I. B. Kuffner, L. J. Walters, M. A. Becerro, V. J. Paul, R. Ritson-Williams, K. S. Beach, Inhibition of coral recruitment by macroalgae and cyanobacteria. *Mar. Ecol. Prog. Ser.* **323**, 107–117 (2006).
16. K. E. Fabricius, M. Logan, S. Weeks, J. Brodie The effects of river run-off on water clarity across the central Great Barrier Reef. *Mar. Pollut. Bull.* **84**, 191–200 (2014).
17. K. E. Fabricius, M. Logan, S. J. Weeks, S. E. Lewis, J. Brodie, Changes in water clarity in response to river discharges on the Great Barrier Reef continental shelf: 2002–2013. *Estuar. Coast. Shelf Sci.* **173**, A1–A15 (2016).
18. G. De'ath, J. M. Lough, K. E. Fabricius, Declining coral calcification on the Great Barrier Reef. *Science* **323**, 116–119 (2009).
19. R. Albright, L. Caldeira, J. Hosfelt, L. Kwiatkowski, J. K. Maclaren, B. M. Mason, Y. Nebuchina, A. Ninokawa, J. Pongratz, K. L. Ricke, T. Rivlin, K. Schneider, M. Sesboüé, K. Shamberger, J. Silverman, K. Wolfe, K. Zhu, K. Caldeira, Reversal of ocean acidification enhances net coral reef calcification. *Nature* **531**, 362–365 (2016).
20. N. E. Cantin, A. L. Cohen, K. B. Karnauskas, A. M. Tarrant, D. C. McCorkle Ocean warming slows coral growth in the central Red Sea. *Science* **329**, 322–325 (2010).
21. A. M. Jones, R. Berkelmans, M. J. H. van Oppen, J. C. Mieog, W. Sinclair, A community change in the algal endosymbionts of a scleractinian coral following a natural bleaching event: Field evidence of acclimatization. *Proc. R. Soc. B* **275**, 1359–1365 (2008).
22. J.-C. Ortiz, M. González-Rivero, P. J. Mumby, An ecosystem-level perspective on the host and symbiont traits needed to mitigate climate change impacts on Caribbean coral reefs. *Ecosystems* **17**, 1–13 (2013).
23. J.-C. Ortiz, M. González-Rivero, P. J. Mumby, Can a thermally tolerant symbiont improve the future of Caribbean coral reefs? *Glob. Chang. Biol.* **19**, 273–281 (2013).
24. G. Roff, E. C. E. Kvennefors, K. E. Ulstrup, M. Fine, O. Hoegh-Guldberg, Coral disease physiology: The impact of Acroporid white syndrome on *Symbiodinium*. *Coral Reefs* **27**, 373–377 (2008).
25. J. A. Maynard, K. R. N. Anthony, C. D. Harvell, M. A. Burgman, R. Beeden, H. Sweatman, S. F. Heron, J. B. Lamb, B. L. Willis, Predicting outbreaks of a climate-driven coral disease in the Great Barrier Reef. *Coral Reefs* **30**, 485–495 (2011).
26. P. J. Mumby, R. Vitolo, D. B. Stephenson, Temporal clustering of tropical cyclones and its ecosystem impacts. *Proc. Natl. Acad. Sci. U.S.A.* **108**, 17626–17630 (2011).
27. N. H. Wolff, A. Wong, R. Vitolo, K. Stolberg, K. R. N. Anthony, P. J. Mumby, Temporal clustering of tropical cyclones on the Great Barrier Reef and its ecological importance. *Coral Reefs* **35**, 613–623 (2016).
28. F. J. Kroon, P. M. Kuhnert, B. L. Henderson, S. N. Wilkinson, A. Kinsey-Henderson, B. Abbott, J. E. Brodie, R. D. R. Turner, River loads of suspended solids, nitrogen, phosphorus and herbicides delivered to the Great Barrier Reef lagoon. *Mar. Pollut. Bull.* **65**, 167–181 (2012).
29. F. J. Kroon, P. Thorburn, B. Schaffelke, S. Whitten, Towards protecting the Great Barrier Reef from land-based pollution. *Glob. Chang. Biol.* **22**, 1985–2002 (2016).
30. W. Large, S. Pond, Open ocean momentum flux measurements in moderate to strong winds. *J. Phys. Oceanogr.* **11**, 324–336 (1981).
31. E. R. Selig, K. S. Casey, J. F. Bruno, New insights into global patterns of ocean temperature anomalies: Implications for coral reef health and management. *Glob. Ecol. Biogeogr.* **19**, 397–411 (2010).
32. A. E. Strong, G. Liu, W. Skirving, C. M. Eakin, NOAA's Coral Reef Watch program from satellite observations. *Ann. GIS* **17**, 83–92 (2011).
33. I. Miller, M. Jonker, G. Coleman, *Crown-of-Thorns Starfish and Coral Surveys Using the Manta Tow and SCUBA Search Techniques* (Australian Institute of Marine Science Townsville, 2003).
34. M. Devlin, B. Schaffelke Spatial extent of riverine flood plumes and exposure of marine ecosystems in the Tully coastal region, Great Barrier Reef. *Mar. Freshwater Res.* **60**, 1109–1122 (2009).
35. M. J. Devlin, C. Petus, E. da Silva, D. Tracey, N. H. Wolff, J. Waterhouse, J. Brodie, Water quality and river plume monitoring in the Great Barrier Reef: An overview of methods based on ocean colour satellite data. *Remote Sens.* **7**, 12909–12941 (2015).

Acknowledgments: We would like to thank M. G. Cabrera for help editing the figures. **Funding:** Funding was provided by a National Environmental Research Program grant to P.J.M. and K.R.N.A., a Pew Fellowship to P.J.M., and an Advance Queensland Fellowship to J.-C.O. **Author contributions:** J.-C.O. and N.H.W. designed and performed the analysis and wrote the manuscript. P.J.M. helped design the study and helped write the manuscript. K.R.N.A. helped design the study and provided feedback on the manuscript. M.D. and S.L. provided environmental data and feedback on the manuscript. **Competing interests:** All authors declare that they have no competing interests. **Data and materials availability:** All data needed to evaluate the conclusions in the paper are present in the paper and/or the Supplementary Materials. Additional data related to this paper may be requested from the authors.

Submitted 29 November 2017
Accepted 12 June 2018
Published 18 July 2018
10.1126/sciadv.aar6127

Citation: J.-C. Ortiz, N. H. Wolff, K. R. N. Anthony, M. Devlin, S. Lewis, P. J. Mumby, Impaired recovery of the Great Barrier Reef under cumulative stress. *Sci. Adv.* **4**, eaar6127 (2018).